World J Microbiol Biotechnol (2014) 30:1819–1827
DOI 10.1007/s11274-014-1608-1

ORIGINAL PAPER

Improvement of catalytic efficiency and thermostability of recombinant *Streptomyces griseus* trypsin by introducing artificial peptide

Zhenmin Ling · Zhen Kang · Yi Liu · Song Liu · Jian Chen · Guocheng Du

Received: 2 September 2013 / Accepted: 17 January 2014 / Published online: 24 January 2014

Abstract *Streptomyces* trypsin is one of the serine proteinases in *Streptomyces griseus* and acts as a key mediator during cell growth and differentiation. *S. griseus* trypsin (SGT) could be successfully expressed in *Pichia pastoris* by engineering the natural propeptide APNP. In this study, the recombinant Exmt with peptide YVEF and the wild-type SGT were comparatively investigated in detail. The recombinant Exmt showed significantly increased thermostability which $t_{1/2}$ value was 3.89-fold of that of the SGT at 40 °C. Moreover, the catalytic efficiency (referring to the specificity constant, k_{cat}/K_m) and pH tolerance of Exmt were also improved. In silico modeling analysis uncovered that introduction of the peptide YVEF resulted in a broadened substrate binding pocket and closer catalytic triad (His^{57}, Asp^{102} and Ser^{195}). The intramolecular Hydrogen bonds and the cation π-interactions were also dramatically increased. The results indicated that engineering of the N-terminus with artificial peptides might be an effective approach for optimizing the properties of the target enzymes.

Keywords Trypsin · Peptide · Catalytic efficiency · Thermostability

Z. Ling · Z. Kang · Y. Liu · S. Liu
The Key Laboratory of Industrial Biotechnology, Ministry of Education, Jiangnan University, Wuxi 214122, China

Z. Ling · Z. Kang (✉) · Y. Liu · S. Liu · J. Chen · G. Du (✉)
School of Biotechnology, Jiangnan University, 1800 Lihu Avenue, Wuxi 214122, China
e-mail: zkang@jiangnan.edu.cn

G. Du
e-mail: gcdu@jiangnan.edu.cn

J. Chen
National Engineering Laboratory for Cereal Fermentation Technology, Jiangnan University, Wuxi 214122, China

G. Du
The Key Laboratory of Carbohydrate Chemistry and Biotechnology, Ministry of Education, Jiangnan University, Wuxi 214122, China

Introduction

Bacterial *Streptomyces griseus* trypsin (SGT) (EC 3.4.21.4) is one of the serine proteinases and acts as a key mediator during cell growth and differentiation (Oh et al. 2007). Due to its wide potential applications in leather bating, food processing, pharmacy, clinical diagnoses and biochemical tests (Ling et al. 2012), SGT has been studied and heterologously produced in *S. lividans* (Choi et al. 2001). In nature, SGT is produced as a zymogen, which consists of a propeptide APNP and a single chain polypeptide of 223 amino acid residues (Chi et al. 2009). Activation of the trypsinogen involves the removal of the N-terminal propeptide at the Pro^4-Val^5 peptide bond (Fig. 1c) (Olafason and Smillie 1975; Kim et al. 1991). Generally, it was accepted that this activation process is non-autocatalytic because of the existence of proline (Kim et al. 1991).

Recently, we have successfully overexpressed the SGT in *Pichia pastoris* (Ling et al. 2012) by introduction of a non-natural peptide YVEF (Fig. 1b) at the N-terminus which caused by digestion with the restriction enzymes *Sna*BI and *Eco*RI (Fig. 1a) and cleavage of the α-factor signal peptide by peptidases KEX2 and STE13 (Brake et al. 1984; Werten and de Wolf 2005; Vadhana et al. 2013). Applying in silico analysis we rationally engineered SGT to improve its activity by modifying the N-terminal peptide (Ling et al. 2013). Therefore, it could be concluded that the

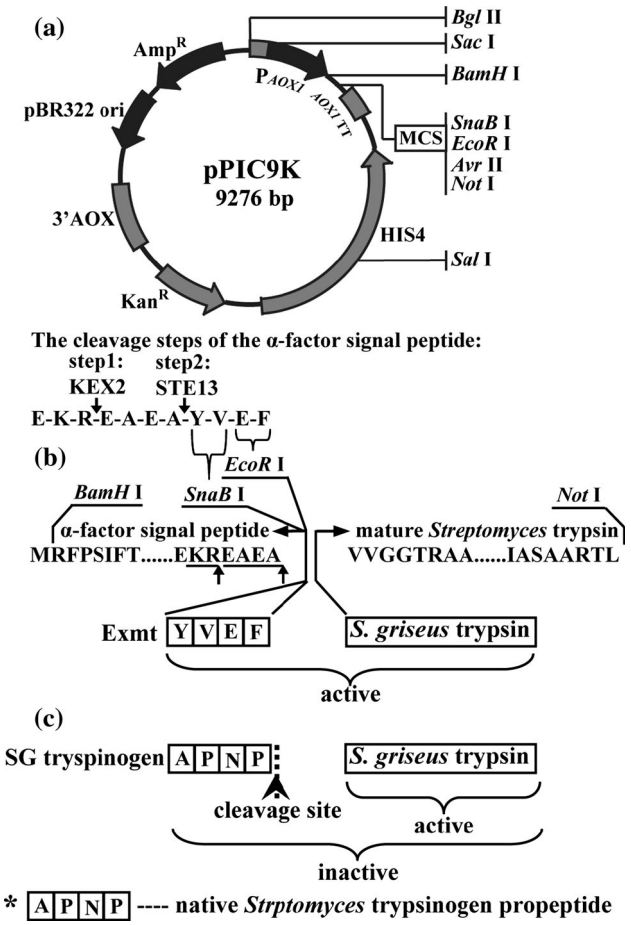

Fig. 1 Schematic representations of vector construction, composition of the wild-type SGT and the recombinant Exmt with the peptide YVEF. **a** The cleavage process of the α-factor signal peptide; **b** composition of the recombinant Exmt; **c** composition of the SGT zymogen

N-terminal peptide plays a crucial role in its activity regulation. Over the past years, many short peptides were discovered, designed and utilized for improving enzyme properties. By engineering the N-terminal residues, the internal packing in polar surface area fraction (Vogt and Argos 1997), the inner molecular interaction between the N-terminal domain (Richter et al. 2002), the substrate binding pocket (Blanchard et al. 1999) and the numbers of the hydrogen (H) bonds (Vogt et al. 1997) could be significantly influenced. Applying this approach, many enzymes were improved in terms of the catalytic efficiency and thermostability (Zhao et al. 2006; Ge et al. 2010; Dai et al. 2012; Yang et al. 2013).

In the present work, the recombinant *Streptomyces* trypsin Exmt produced by *P. pastoris* and its wild-type SGT from *S. griseus* were deeply and comparatively investigated with respect to the catalytic efficiency and thermostability. Compared with SGT, the recombinant Exmt showed significantly increased catalytic efficiency and thermostability. To uncover the key parameters involved these remarkable changes, the three-dimensional (3D) structure of the recombinant Exmt was also constructed in silico and compared with the SGT crystal structure.

Materials and methods

Microorganisms and growth conditions

Streptomyces griseus ATCC 10137^{TM} which producing the wild-type SGT was purchased from the American Type Culture Collection (ATCC, USA). The R2YE liquid broth was used for cultivation of *S. griseus* ATCC 10137^{TM} (Chi et al. 2009). *P. pastoris* GS115 and plasmid pPIC9 K were both purchased from the Invitrogen company. The recombinant plasmid pPIC9 K-Exmt and strain GS115/pPIC9 k-Exmt were constructed previously (Ling et al. 2012). Yeast nutrient medium: minimal dextrose medium, minimal medium, yeast extract peptone dextrose medium, buffered minimal glycerol-complex medium and buffered minimal methanol-complex medium were prepared by means of "*P. pastoris* expression Kit" (Pichia Multi-Copy Expression Kit, version A, Invitrogen BV, The Netherlands.).

Expression and purification of SGT and Exmt

Stock of *S. griseus* ATCC10137^{TM} spore suspensions was used to inoculate 25 ml of R2YE liquid medium in 250 ml baffled flasks. After incubation at 28 °C with vigorous shaking at 200 rpm for 48 h, 1 ml of the culture broth was transferred to 500 ml baffled flask with 100 ml of fresh R2YE liquid medium. After 24 h of cultivation under the same conditions, 1 ml culture broth was taken every 24 h and the supernatant was used for determination of trypsin amidase activity.

The *P. pastoris* transformant was cultured in 250 ml baffled flask supplied with 25 ml buffered glycerol-complex medium at 30 °C at an agitation of 250 rpm. When the culture reached an OD_{600} value of about 4.0, the cells were centrifuged and resuspended in 30 ml of buffered methanol-complex medium to an OD_{600} value of 1.0, and shaken at 30 °C at an agitation of 250 rpm in 250 ml baffled flasks for 144 h. The culture broth was supplemented with methanol (10 g l^{-1}) every 24 h to induce the expression of recombinant Exmt.

SGT and Exmt were purified with the same procedures. The crude sample was concentrated by precipitation with 25–55 % ammonium sulfate. Then the precipitate was resuspended in 5 ml buffer A (10 mM Tris–HCl, pH 8.0, 10 % (w/v) glycerol, and 1 mM EDTA) and dialyzed overnight against 100 ml of the same buffer. The sample was loaded onto a Hitrap benzamidine FF column

(Φ1.6 × 2.5 cm, GE Healthcare, catalog number 17-5144-01) previously equilibrated with buffer A, and the column was washed with buffer B (10 mM NaOAc, pH 5.0, 10 % glycerol, 1 mM EDTA, and 0.5 M NaCl). Proteins were eluted with 6 M guanidine chloride solution at a flow rate of 2.5 ml min^{-1}, and fractions containing trypsin activity were collected and dialyzed against buffer A. Protein concentration was estimated by a Coomassie Brilliant Blue R-250 binding assay (Bradford 1976), using a commercial standard protein solution containing bovine G-globulin. Protein concentration of effluents was monitored at 280 nm.

SDS-PAGE analysis of the SGT and Exmt

The protein was fractionated by SDS-PAGE system as described by Hu (Hu et al. 2012). 30 µl samples were pretreated by mixing with 5 µl 5× SDS-PAGE loading buffer in a 0.5 ml centrifugal tube. The samples were incubated at 100 °C for 10 min, and then each sample aliquot (10 µl) was loaded into the sample well. The proteins were separated using 12 % SDS–polyacrylamide gels and stained with Coomassie brilliant blue.

Determination of trypsin activity with different substrates

Trypsin activity was determined and characterized as amidase and esterase activities with the artificial substrates N_α-benzoyl-DL-arginine-*p*-nitroanilide (BAPNA) and N_α-benzoyl-L-arginine ethyl ester hydrochloride (BAEE), respectively. The detailed process was described previously (Ling et al. 2012).

Effects of temperature on trypsin activity and stability

To determine the optimum temperature, the enzyme was analyzed from 10 to 70 °C in 50 mM Tris–HCl buffer (pH 8.0). The relative activities (%) at other temperatures were obtained by comparing with the highest activity for the same enzyme. The thermostability of trypsin was determined at the elevated temperatures (40, 50 and 60 °C). The trypsin amidase activity was measured as described above and the rates were reported as percentage of the initial rates. The relative amidase activities were compared at 40 °C every 30 min and at 50 and 60 °C every 5 min. The initial trypsin amidase activity was taken as 100 %.

Half-life determination

The half-lives of Exmt and SGT in the purification buffer were obtained by fitting the relative activity to a single exponential equation with three parameters (Eq. 1), and then calculated as Eq. 2

$$y = y_0 + a\exp(-bx) \quad (1)$$

$$t_{1/2} = \frac{\ln 2}{b} \quad (2)$$

Effects of pH on trypsin activity and stability

In order to estimate the optimum pH of SGT and Exmt, the purified protein was incubated in Britton-Robinson Buffer (pH 2.0–12.0, 40 mM H_3BO_3, 40 mM H_3PO_4, and 40 mM CH_3COOH). The amidase activity determined at a certain pH was taken as 100 %. The pH stability of trypsin was determined at pH ranging from 2.0 to 12.0 at 37 °C for 1 h. After incubation in Britton-Robinson Buffer (pH 2.0–12.0). The trypsin activity was measured at pH 8.0 at 37 °C. The highest residual activity at a certain pH was taken as 100 %.

Determination of kinetic parameters

Kinetic parameters towards BAPNA were evaluated with 50 mM Tris–HCl buffer (pH 8.0) at 37 °C. For Michaelis–Menten kinetics, 11 concentrations (0.01, 0.02, 0.03, 0.04, 0.05, 0.06, 0.07, 0.08, 0.09, 0.10, 0.12) of BAPNA (dissolved in DMF) were used and at least one concentration above and below the K_m value. Kinetic parameters towards BAEE were evaluated with 67 mM K_2HPO_4–KH_2PO_4 buffer (pH 7.6) at 25 °C. For Michaelis–Menten kinetics, ten concentrations (0.0125, 0.015, 0.02, 0.025, 0.05, 0.1, 0.125, 0.15, 0.20, 0.25) of BAEE (dissolved in 67 mM K_2HPO_4–KH_2PO_4 buffer, pH 7.6) were used and at least one concentration above and below the K_m value.

Template selection for construction of 3D model structure

The X-ray crystal structure of SGT (PDB ID: 1sgt) was downloaded from the RCSB Protein Data Bank (http://www.pdb.org/pdb/home/home.do). Note that in this paper we use the original residue numbers reported in the literature and 1sgt PDB file, while the corresponding residue numbers in 1sgt PDB file are not shifted by adding extra amino acids at its N-terminal (Table 1). Due to the lack of detailed and mechanical knowledge about propeptide and trypsinogen, the structure of SGT was used as the template for modeling. Stereo chemical analysis of the structure was performed using the online server PROCHECK (http://nihserver.mbi.ucla.edu/SAVS/), and the final model which displaying good geometry with less than 1 % of residues in the disallowed region was used in the present study.

Modeling procedure of the recombinant Exmt

The coordinates used for the molecular dynamics procedure were obtained from previous modeling steps. The 3D

Table 1 Enzyme properties of the wild-type SGT and the recombinant Exmt

Properties	SGT	Exmt
Optimum pH	8.0	8.0
Optimum Tm (°C)	50	50
Specific activity ($\times 10^3$ U mg^{-1})	0.56 ± 0.02	0.55 ± 0.07
K_m ($\times 10^{-5}$ mol l^{-1}, substrate BAPNA)	9.24 ± 0.06	5.69 ± 0.09
k_{cat} ($\times 10^3$ min^{-1}, substrate BAPNA)	0.90 ± 0.02	0.67 ± 0.05
k_{cat}/K_m ($\times 10^7$ mol^{-1} l min^{-1}, substrate BAPNA)	0.98 ± 0.03	1.17 ± 0.08
K_m ($\times 10^{-5}$ mol l^{-1}, substrate BAEE)	7.29 ± 0.09	2.15 ± 0.07
k_{cat} ($\times 10^4$ min^{-1}, substrate BAEE)	1.14 ± 0.01	0.53 ± 0.07
k_{cat}/K_m ($\times 10^8$ mol^{-1} l min^{-1}, substrate BAEE)	1.56 ± 0.03	2.49 ± 0.05
$t_{1/2}$ (40 °C min^{-1})	57.12 ± 0.90	221.92 ± 11.69

model structure was constructed by the software NAMD with charm M force field (http://www.ks.uiuc.edu/Research/namd) (Phillips et al. 2005). Na^+ was added to neutralize the system and pH 7.0 was set as default. Proteins were solvated in a cubic box consisting of TIP3P water molecules, and the box size was chosen according to the criterion that the distance of protein atoms from the wall was greater than 10.0 Å. An Ewald summation method was used for calculating the total electrostatic energy in a periodic box named Particle Mesh Ewald. Structure minimization was performed to remove any unexpected coordinate collision and get the local minima. The water box and the whole system were minimized using the descent method plus the conjugate gradient method. After minimization, the system heating, equilibration and data sampling were carried out in turn. The system heating was performed gradually from 0 K to the desired temperature in a NTV ensemble, followed by a further 150 ps simulation for equilibration and 3 ns or longer simulation for data sampling in a NTP ensemble. The temperature was set as 300 and 330 K, respectively at 1 atm. pressure. Finally, the structural diagram was drawn with PyMOL software (http://pymol.sourceforge.net/).

Parameters calculation of the protein structure

The amino acids (primary structural parameter), intramolecular H bonds, ion pairs, and the cation π-interactions (secondary structural parameters), and secondary structure contents (tertiary structural parameter) are the key points for further investigation. The amino acids were calculated by the Vector NTI software. The intramolecular H bonds were predicted by the software PyMOL (http://pymol.sourceforge.net/). The cation π-interactions were predicted by the online program CaPTURE (http://capture.caltech.edu/) (Gallivan and Dougherty 1999) (Fig. 2).

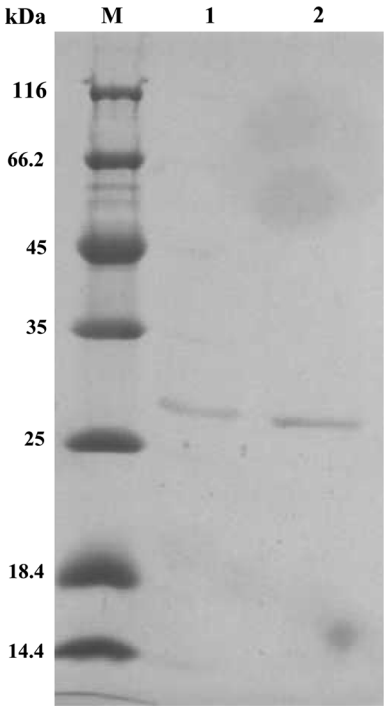

Fig. 2 SDS–PAGE analysis of the purified SGT and the recombinant Exmt with the peptide YVEF. M, marker; *lane* 1, purified SGT; *lane* 2, purified Exmt

Results

Increased thermostability with the peptide YVEF

The effects of temperature on the activity and the stability were determined and compared between the wild-type SGT and the recombinant Exmt. As shown in Fig. 3c, both SGT and Exmt showed the same optimum temperature (50 °C). However, compared with SGT, the recombinant Exmt exhibited notably increased thermostability. When treated at 40 °C for 60 min, Exmt was completely stable while SGT remained only 36 % residual activity (Fig. 3d). After incubation for 360 min, about 50 and 7 % residual

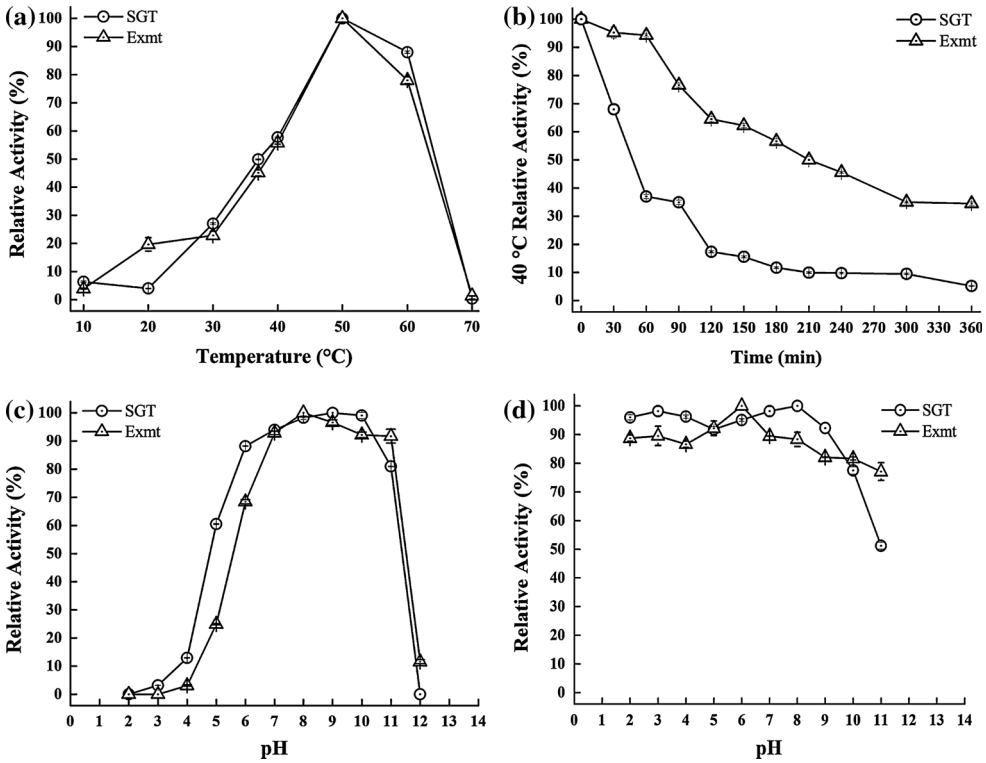

Fig. 3 Influence of temperature and pH on activities of the wild-type SGT and the recombinant Exmt with the peptide YVEF. **a** Temperature kinetics of the SGT and Exmt; **b** thermostability of SGT and Exmt at 40 °C; **c** pH kinetics of SGT and Exmt; **d** pH tolerance of SGT and Exmt

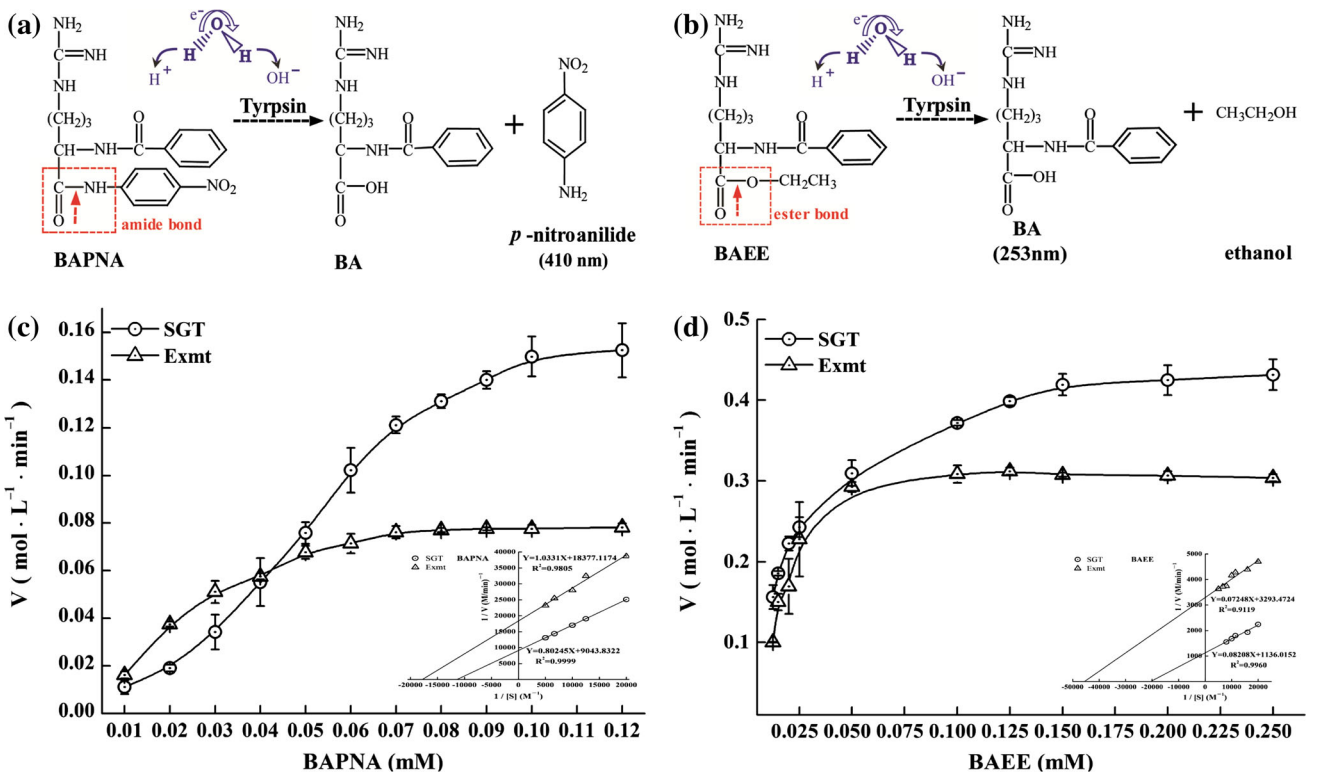

Fig. 4 Enzymatic reaction kinetics of the wild-type SGT and the recombinant Exmt with the peptide YVEF. **a** Enzymatic reaction with amidase substrate N_{α}-benzoyl-DL-arginine-*p*-nitroanilide (BAPNA); **b** enzymatic reaction with esterase substrate N_{α}-benzoyl-L-arginine ethyl ester hydrochloride (BAEE); **c** Michaelis–Menten and Lineweaver–Burk reciprocal plots of SGT and Exmt with amidase substrate BAPNA; **d** Michaelis–Menten and Lineweaver–Burk reciprocal plots of SGT and Exmt with esterase substrate BAEE

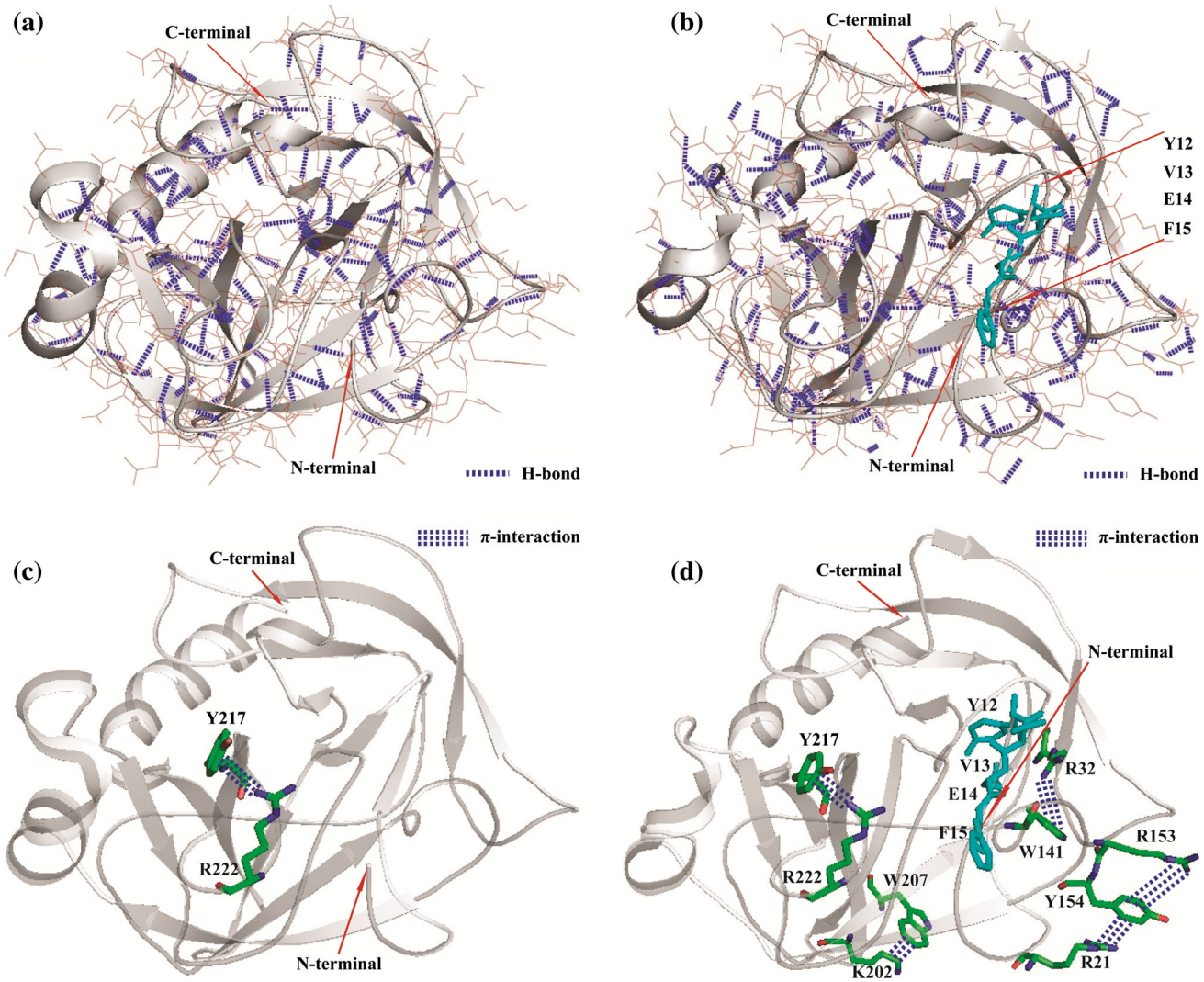

Fig. 5 Networks of the intramolecular H bonds and the cation π-interactions in the wild-type SGT and the recombinant Exmt with the peptide YVEF. **a** Network of the intramolecular H bonds in the wild-type SGT; **b** network of the intramolecular H bonds in the recombinant Exmt; **c** cation π-interactions of the wild-type SGT; **d** cation π-interactions of the recombinant Exmt. The sticks are designated as peptides

activities were detected for Exmt and SGT, respectively. Moreover, when incubating at 50 and 60 °C for 10 min, Exmt remained approximate 5 % residual activity whereas SGT was thoroughly inactive (data not shown). In parallel, the thermal half-life ($t_{1/2}$) values of SGT and Exmt were also investigated and compared. As shown in Table 1, the $t_{1/2}$ value of the recombinant Exmt at 40 °C were 222 min which was 3.89-fold of that of SGT. The results demonstrated that the N-terminal peptide YVEF plays an important role in modulation of the thermostability.

Increased alkaline stability with the peptide YVEF

The influence of pH on the trypsin activity was determined in the range of pH 2.0–12.0 in the Britton-Robinson Buffer. As shown in Fig. 3c, the wild-type SGT showed a broad pH interval (from pH 6.0 to 10.0), whereas the recombinant Exmt represented an alkaline shift (from pH 7.0 to 11.0). The optimum pH of SGT and Exmt were approximately same as pH 8.0. Furthermore, the influence of pH on the trypsin stability was also determined. As shown in Fig. 3d, Exmt exhibited more stability than SGT in the range of pH 10.0–11.0. These results suggested that the peptide YVEF not only improved the pH tolerance but also gave rise to an alkaline shift.

Effect of the peptide YVEF on kinetic parameters and catalytic efficiency

The effect of the peptide YVEF on kinetic parameters and catalytic efficiency were comparatively analyzed with the

substrates BAPNA (amidase substrate) and BAEE (esterase substrate) (Fig. 4a, b). As shown in Fig. 4c, d, both SGT and Exmt exhibited normal Michaelis–Menten kinetics according to the Lineweaver–Burk curves with substrates BAPNA and BAEE. Compared with SGT, the recombinant Exmt showed decreased values of K_m with both substrates BAPNA and BAEE (Table 1), indicating that increased substrate affinity. As a consequence, Exmt showed an increased catalytic efficiency (k_{cat}/K_m) although both values of V_{max} and k_{cat} were decreased.

Simulation and analysis of the 3D-model structure

In vitro investigations combining with in silico simulation are always the common method for improving the enzyme properties (Zhang et al. 2010, 2011). To investigate the influence of the peptide YVEF on the trypsin properties from a structural perspective, the 3D model structure of Exmt (Fig. 5b) was constructed according to SGT crystal structure (PDB ID: 1sgt, Fig. 5a) with a root mean square deviation value of 0.69. Compared to SGT, Exmt showed an expanding substrate binding pocket (D^{189}, G^{216}–G^{226} loop) with a longer C_α-distance between G^{216} and G^{226} (10.56 Å) (Fig. 5c). As a consequence, substrates would be easier to enter this crevice and interact with the residue Asp^{189} (Kraut 1977), which eventually resulted increased substrate affinity.

In addition, the distance among the catalytic triad of Exmt also decreased (Fig. 5c, d), indicating that a better catalytic distance and catalytic efficiency were generated.

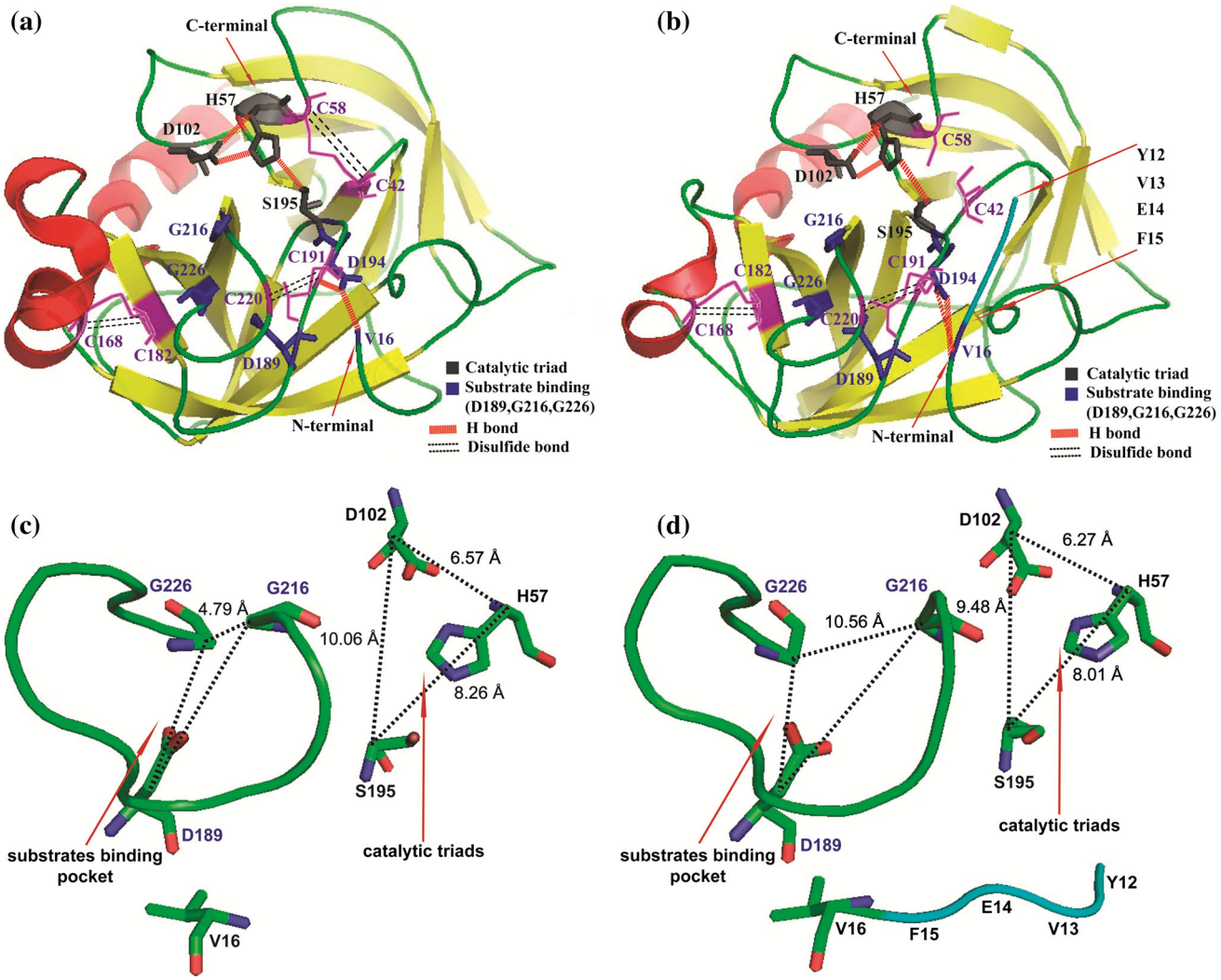

Fig. 6 Construction of the 3D model structure of the recombinant *S. griseus* trypsin Exmt with the software NAMD. The crystal structure of SGT was used as the template. **a** Crystal structure of the wild-type SGT; **b** simulated structure of the recombinant Exmt; **c** C_α-distances of the substrate binding pocket and catalytic triad in the wild-type SGT; **d** C_α-distances of the substrate binding pocket and catalytic triad in the recombinant Exmt

Although the k_{cat} value of Exmt declined which might be caused by the altered rigidity, the k_{cat}/K_m value was inversely increased because of bigger substrate affinity. Previously, different groups have demonstrated that intramolecular H bonds and cation π-interactions are important for the trypsin stability (Kraut 1977; Gallivan and Dougherty 1999; Lee et al. 2004). Hence, the intramolecular H bonds and the cation π-interactions were also calculated and comparatively investigated. Apparently, Exmt contained 312 intramolecular H bonds (Fig. 6b) and five cation π-interactions (Fig. 6d), which were more than those of SGT (251 intramolecular H bonds and Fig. 6a; one cation π-interactions, Fig. 6c).

Discussion

Streptomyces trypsin, a representative of serine proteases, has been attracted intensive studies. Similar with the bovine trypsin, its activation also involves in removal of the N-terminal propeptide (Chen et al. 2003; Ling et al. 2012). However, the activation mechanism of the *Streptomyces* trypsin was considered to be different from that of the bovine trypsin (Olafson et al. 1975; Kim et al. 1991). Recently, we constructed a series of variants with different peptides and successfully achieved its active expression with the *P. pastoris* system. More importantly, the results demonstrated that natural propeptide APNP plays a key role in inhibiting the *Streptomyces* trypsin activity (Ling et al. 2012). In addition, although no trypsin activity was detected in the culture of the recombinant with the mammal trypsin propeptide VDDDDK, notable activity was recovered after digestion with enterokinase which further confirmed the importance of the N-terminus. Therefore, in the present work, we investigated the properties of the constructed recombinant Exmt with the peptide YVEF (Ling et al. 2012).

In recent years, many types of N-terminal peptides have been designed to improve the expression level or the properties of the target enzymes (Liu et al. 2006; Ge et al. 2010; Dai et al. 2012; Rajput et al. 2012; Yang et al. 2013). Here, compared with SGT, Exmt showed notably increased thermostability (Fig. 3b). In general, it was accepted that many factors such as H bonds and cation-π interactions are closely connected to the thermostability (Gallivan and Dougherty 1999). As shown in Fig. 5, both numbers of the intramolecular H bonds and the cation-π interactions were remarkably increased in Exmt. Moreover, the pH tolerance was also improved (Fig. 3d) which was similar with recent report (Huang et al. 2012).

In addition to the stability, the peptide YVEF also displayed a crucial role in the regulation of the catalytic efficiency (Fig. 4c, d). In fact, many short amphipathic peptides have been investigated for improving the catalytic efficiency of the recombinant enzymes, which might be ascribed to the influence of the N-terminal sequence on substrate binding ability, rigidity or stereoselectivity of the enzymes (Mollania et al. 2011; Mosbah et al. 2010). Focused on the *Streptomyces* trypsin, it has been demonstrated that different N-terminal peptides including the natural propeptide APNP play curial roles in its activity regulation (Zhang et al. 2007; Charbonneau et al. 2012). Introduction of the peptide YVEF broadened the substrate binding pocket (Fig. 6c, d) and changed the surrounding environment, which eventually resulted increased substrate binding ability and catalytic efficiency (Kraut 1977; Page et al. 2003). Compared with SGT, Exmt showed a closer catalytic triad (His^{57}, Asp^{102}, Ser^{195}), which might also increase the catalytic efficiency (Stroud et al. 1977; Rypniewski et al. 1994).

In conclusion, the non-natural peptide YVEF introduced at the N-terminus of SGT played significant roles in regulation of its enzyme properties. Compared with SGT, Exmt showed higher catalytic efficiency (represented as k_{cat}/K_m value), pH tolerance and thermostability. In silico modeling analysis results illustrated that compared with SGT, Exmt showed an enlarged substrate binding pocket and a closer catalytic triad. Moreover, the hydrogen bonds and the cation π-interactions were both notably increased in Exmt. Taken together, it might be applicable for optimizing the properties of the target enzyme by modification of the N-terminal peptide.

Acknowledgments This work was financially supported by the National High Technology Research and Development Program of China (863 Program, 2011AA100905), Program for Changjiang Scholars and Innovative Research Team in University (No. IRT1135), the National Natural Science Foundation of China (31200020, 31000031), the National Science Foundation for Post-doctoral Scientists of China (2013M540414) and the Jiangsu Planned Projects for Postdoctoral Research Funds (1301010B), the Doctor Candidate Foundation of Jiangnan University (JUDCF10014), the 111 Project and the Priority Academic Program Development of Jiangsu Higher Education Institutions.

References

Blanchard CZ, Chapman-Smith A, Wallace JC, Waldrop GL (1999) The biotin domain peptide from the biotin carboxyl carrier protein of *Escherichia coli* acetyl-CoA carboxylase causes a marked increase in the catalytic efficiency of biotin carboxylase and carboxyltransferase relative to free biotin. J Biol Chem 274(45):31767–31769

Bradford MM (1976) A rapid and sensitive method for the quantitation of microgram quantities of protein utilising the principle of protein-dye binding. Anal Biochem 72:248–254

Brake AJ, Merryweather JP, Coit DG, Heberlein UA, Masiarz FR, Mullenbach GT, Urdea MS, Valenzuela P, Barr PJ (1984) Alpha-factor-directed synthesis and secretion of mature foreign proteins in *Saccharomyces cerevisiae*. Proc Natl Acad Sci USA 81(15):4642–4646

Charbonneau DM, Meddeb-Mouelhi F, Beauregard M (2012) N-terminal purification tag alters thermal stability of the carboxylesterase EstGtA2 from *G. thermodenitrificans* by impairing reversibility of thermal unfolding. Protein Pept Lett 19(3):264–269

Chen JM, Kukor Z, Le Marechal C, Toth M, Tsakiris L, Raguenes O, Ferec C, Sahin-Toth M (2003) Evolution of trypsinogen activation peptides. Mol Biol Evol 20(11):1767–1777

Chi W-J, Song J-H, A. Oh E, Park S-W, Chang YK, Kim E-S, Hong S-K (2009) Medium optimization and application of an affinity column chromatography for *Streptomyces griseus* trypsin production from the recombinant *Streptomyces griseus*. J Microbiol Biotechnol 19(10):1191–1196

Choi SS, Chi WJ, Lee JH, Kang SS, Jeong BC, Hong SK (2001) Overexpression of the *sprD* gene encoding *Streptomyces griseus* protease D stimulates actinorhodin production in *Streptomyces lividans*. J Microbiol 39(4):305–313

Dai Z, Fu HT, Zhang YF, Zeng J, Tang B, Tang XF (2012) Insights into the maturation of hyperthermophilic pyrolysin and the roles of its N-terminal propeptide and long C-terminal extension. Appl Environ Microbiol 78(12):4233–4241

Gallivan JP, Dougherty DA (1999) Cation-π interactions in structural biology. Proc Natl Acad Sci USA 96(17):9459–9464

Ge B, Yang F, Yu D, Liu S, Xu H (2010) Designer amphiphilic short peptides enhance thermal stability of isolated photosystem-I. PloS One 5(4):e10233. doi:10.1371/journal.pone.0010233

Hu HY, Yang JC, Chen JH, Chi MC, Lin LL (2012) Enzymatic characterization of *Bacillus licheniformis* gamma-glutamyltranspeptidase fused with N-terminally truncated forms of Bacillus sp TS-23 alpha-amylase. Enzym Microb Technol 51(2):86–94

Huang SY, Zhang YHP, Zhong JJ (2012) A thermostable recombinant transaldolase with high activity over a broad pH range. Appl Microbiol Biotechnol 93(6):2403–2410

Kim JC, Cha SH, Jeong ST, Oh SK, Byun SM (1991) Molecular cloning and nucleotide sequence of *Streptomyces griseus* trypsin gene. Biochem Biophys Res Commun 181(2):707–713

Kraut J (1977) Serine proteases: structure and mechanism of catalysis. Annu Rev Biochem 46:331–358

Lee WS, Park CH, Byun SM (2004) *Streptomyces griseus* trypsin is stabilized against autolysis by the cooperation of a salt bridge and cation-π interaction. J Biochem 135(1):93–99

Ling Z, Ma T, Li J, Du G, Kang Z, Chen J (2012) Functional expression of trypsin from *Streptomyces griseus* by *Pichia pastoris*. J Ind Microbiol Biotechnol 39(11):1651–1662

Ling ZM, Liu Y, Teng SL, Kang Z, Zhang JJ, Chen J, Du GC (2013) Rational design of a novel propeptide for improving active production of *Streptomyces griseus* trypsin in *Pichia pastoris*. Appl Environ Microbiol 79(12):3851–3855

Liu G, Tang X, Tian SL, Deng X, Xing M (2006) Improvement of the cellulolytic activity of *Trichoderma reesei* endoglucanase IV with an additional catalytic domain. World J Microb Biotechnol 22(12):1301–1305

Mollania N, Khajeh K, Ranjbar B, Hosseinkhani S (2011) Enhancement of a bacterial laccase thermostability through directed mutagenesis of a surface loop. Enzym Microb Technol 49(5):446–452

Mosbah H, Horchani H, Sayari A, Gargouri Y (2010) The insertion of (LK) residues at the N-terminus of *Staphylococcus xylosus* lipase affects its catalytic properties and its enantioselectivity. Process Biochem 45(5):777–785

Oh EA, Kim MS, Chi WJ, Kim JH, Hong SK (2007) Characterization of the sgtR1 and sgtR2 genes and their role in regulating expression of the *sprT* gene encoding *Streptomyces griseus* trypsin. FEMS Microbiol Lett 276(1):75–82

Olafason RW, Smillie LB (1975) Enzymic and physicochemical properties of *Streptomyces griseus* trypsin. Biochemistry 14(6): 1161–1167

Olafson RW, Jurasek L, R.Carpenter M, B.Smillie L, 1168 (1975) Amino acid sequence of *Streptomyces griseus* trypsin. Cyanogen bromide fragments and complete sequence. Biochemistry 14(6):1168–1177

Page MJ, Wong SL, Hewitt J, Strynadka NCJ, MacGillivray RTA (2003) Engineering the primary substrate specificity of *Streptomyces griseus* trypsin. Biochemistry 42(30):9060–9066

Phillips JC, Braun R, Wang W, Gumbart J, Tajkhorshid E, Villa E, Chipot C, Skeel RD, Kale L, Schulten K (2005) Scalable molecular dynamics with NAMD. J Comput Chem 26(16): 1781–1802

Rajput R, Tiwary E, Sharma R, Gupta R (2012) Swapping of prosequences between keratinases of *Bacillus licheniformis* and *Bacillus pumilus*: altered substrate specificity and thermostability. Enzym Microb Technol 51(3):131–138

Richter K, Reinstein J, Buchner J (2002) N-terminal residues regulate the catalytic efficiency of the Hsp90 ATPase cycle. J Biol Chem 277(47):44905–44910

Rypniewski WR, Perrakis A, Vorgias CE, Wilson KS (1994) Evolutionary divergence and conservation of trypsin. Protein Eng 7(1):57–64

Stroud RM, Kossiakoff AA, Chambers JL (1977) Mechanisms of zymogen activation. Annu Rev Biophys Bioeng 6:177–193

Vadhana AKP, Samuel P, Berin RM, Krishna J, Kamatchi K, Meenakshisundaram S (2013) Improved secretion of *Candida antarctica* lipase B with its native signal peptide in *Pichia pastoris*. Enzym Microb Technol 52(3):177–183

Vogt G, Argos P (1997) Protein thermal stability: hydrogen bonds or internal packing ? Fold Des 2(4):S40–S46

Vogt G, Woell S, Argos P (1997) Protein thermal stability, hydrogen bonds, and ion pairs. J Mol Biol 269(4):631–643

Werten MW, de Wolf FA (2005) Reduced proteolysis of secreted gelatin and Yps1-mediated alpha-factor leader processing in a *Pichia pastoris* kex2 disruptant. Appl Environ Microbiol 71(5):2310–2317

Yang H, Lu X, Liu L, Shin H-d, Chen RR, Li J, Du G, Chen J (2013) Fusion of an oligopeptide at the N-terminus of an alkaline α-amylase from *Alkalimonas amylolytica* simultaneously improves its catalytic efficiency, thermal stability, and oxidative stability. Appl Environ Microbiol 79(9):3049–3058

Zhang FL, Chi ZM, Zhu KL, Li J, Li MJ, Liang LK, Wu LF (2007) Expression in *Escherichia coli* of the recombinant *Vibrio anguillarum* metalloprotease and its purification and characterization. World J Microb Biotechnol 23(3):331–337

Zhang Z, Teng SL, Wang LJ, Schwartz CE, Alexov E (2010) Computational analysis of missense mutations causing Snyder–Robinson syndrome. Hum Mutat 31(9):1043–1049

Zhang Z, Norris J, Schwartz C, Alexov E (2011) In silico and in vitro investigations of the mutability of disease-causing missense mutation sites in spermine synthase. PloS One 6(5):e20373. doi:10.1371/journal.pone.0020373

Zhao XJ, Nagai Y, Reeves PJ, Kiley P, Khorana HG, Zhang SG (2006) Designer short peptide surfactants stabilize G protein-coupled receptor bovine rhodopsin. Proc Natl Acad Sci USA 103(47):17707–17712